Published in final edited form as:
Virology. 2014 August ; 0: 351–362. doi:10.1016/j.virol.2014.06.001.

Each of the eight simian hemorrhagic fever virus minor structural proteins is functionally important

Heather A. Vatter[1], **Han Di**[1], **Eric F. Donaldson**[2], **Ralph S. Baric**[2], and **Margo A. Brinton**[1,*]

[1]Department of Biology, Georgia State University, Atlanta GA 30302

[2]Department of Epidemiology, University of North Carolina at Chapel Hill, Chapel Hill, NC 27599

Abstract

The simian hemorrhagic fever virus (SHFV) genome differs from those of other members of the family *Arterivirus* in encoding two adjacent sets of four minor structural protein open reading frames (ORFs). A stable, full-length, infectious SHFV-LVR cDNA clone was constructed. Virus produced from this clone had replication characteristics similar to those of the parental virus. A subgenomic mRNA was identified for the SHFV ORF previously identified as 2b. As an initial means of analyzing the functional relevance of each of the SHFV minor structural proteins, a set of mutant infectious clones was generated, each with the start codon of one minor structural protein ORF mutated. Different phenotypes were observed for each ortholog of the pairs of minor glycoproteins and all of the eight minor structural proteins were required for the production of infectious extracellular virus indicating that the duplicated sets of SHFV minor structural proteins are not functionally redundant.

Keywords

simian hemorrhagic fever virus; subgenomic mRNAs; minor structural proteins; infectious clone

INTRODUCTION

Simian hemorrhagic fever virus (SHFV) was first identified in the 1960s when it was found to be the causative agent of fatal hemorrhagic fever outbreaks in captive rhesus macaque colonies in the United States, Russia and Europe (Tauraso et al., 1968). Experimental SHFV infections in several macaque species produced clinical symptoms including fever, anorexia, adipsia, cyanosis, skin petechial and nose bleeds and ultimately, led to death by 7 to 13 days after infection (Allen et al., 1968; London, 1977; Palmer et al., 1968). These symptoms closely resembled those induced by other types of hemorrhagic fever viruses, such as Ebola Zaire and Marburg viruses in rhesus macaques (Bray, 2005). Various species of African

*To whom correspondence should be addressed: Georgia State University, Department of Biology P.O. Box 4010 Atlanta, GA, 30303 mbrinton@gsu.edu. Phone: 404-413-5388, Fax: 404-413-5301.

monkeys are the natural hosts of SHFV, and in baboons, vervets, patas monkeys and African green monkeys, SHFV infections are typically asymptomatic and often persistent (Gravell et al., 1986). Previous SHFV outbreaks in macaque colonies are thought to have been caused by inadvertent mechanical transfer of SHFV present in the blood of a persistently infected African monkey to a macaque followed by efficient transmission of the virus between macaques (Palmer et al., 1968). Humans exposed to SHFV-infected macaques did not develop disease symptoms or seroconvert (Dalgard et al., 1992; Palmer et al., 1968).

SHFV is a member of the family *Arteriviridae* that also includes equine arteritis virus (EAV), porcine reproductive and respiratory syndrome virus (PRRSV), lactate dehydrogenase elevating virus (LDV) and wobbly possum disease virus (Dunowska et al., 2012; Snijder and Meulenberg, 1998). The *Arteriviridae*, *Coronaviridae* and *Roniviridae* families are classified within the Order *Nidovirales* based on similarities in genome organization and replication strategy (Snijder and Kikkert, 2013). The SHFV genome is a 5′ capped and 3′ polyadenylated, positive-sense, single-stranded RNA of approximately 15.7 kb. The 5′ two-thirds of the genome encodes the ORF1a and ORF1ab polyproteins (Fig. 1A). The nonstructural proteins proteolytically cleaved from these polyproteins are required for the replication and transcription of the viral genomic and subgenomic (sg) RNAs (Beerens et al., 2007; Snijder and Meulenberg, 1998).

The viral structural proteins are encoded at the 3′ end of the genome and are expressed from a 3′ and 5′ coterminal, nested set of sg mRNAs. The 3′ most gene (ORF7) encodes the 15 kDa nucleocapsid (N) protein which forms disulfide-linked homodimers that interact to form the nucleocapsid (Dea et al., 2000; Snijder and Meulenberg, 1998). The interaction of the basic N-terminal domain of the N protein with genome RNA is thought to facilitate packaging of the viral RNA into the nucleocapsid (Dea et al., 2000). The two other major structural proteins are the 19 kDa non-glycosylated membrane (M) protein and the 26 kDa major glycoprotein (GP5). These two virion envelope-associated proteins interact to form disulfide-linked heterodimers that function in virion attachment (Delputte et al., 2007; Delputte et al., 2002). The M protein is the most conserved arterivirus structural protein and is essential for progeny virion assembly (Delputte et al., 2002; Snijder and Meulenberg, 1998). The macrophage-restricted protein sialoadhesion (CD169) serves as the arterivirus receptor and mediates virion internalization (Van Breedam et al., 2010; Welch and Calvert, 2010), while the macrophage-specific CD163 antigen is required for virion entry/uncoating (Calvert et al., 2007; Van Gorp et al., 2008). Recently, an additional ORF (GP5a) that starts at an alternative AUG within the major glycoprotein GP5 ORF was identified in the genomes of each of the known arteriviruses (Firth et al., 2011). An EAV reverse genetic study indicated that GP5a was not an essential protein but its absence reduced virus yields and GP5a was detected in purified PRRSV particles (Johnson et al., 2011; Sun et al., 2013).

The EAV, PRRSV and LDV genomes also encode four minor structural proteins: E, GP2, GP3 and GP4. The sequences of these proteins are less conserved between different arteriviruses than those of the major structural proteins. The minor structural GPs form complexes located on the surface of virions that are postulated to be involved in receptor binding and virion uncoating (Snijder and Kikkert, 2013). The E protein is translated from bicistronic sg mRNA 2 that also expresses GP2 and it has been proposed that E oligomers

function as ion-channels during virion entry (Lee and Yoo, 2006; Snijder et al., 1999). The SHFV genome encodes two adjacent sets of four minor structural protein ORFs (Godeny et al., 1998).

A stable, full-length cDNA infectious clone for SHFV-LVR (SHFVic) was constructed. The replication characteristics of the virus produced by MA104 cells transfected with *in vitro*-transcribed SHFVic RNA were similar to those of the parental SHFV-LVR virus. A separate sg mRNA was identified for the SHFV ORF previously identified as 2b. A set of mutant infectious clones, each lacking the expression of one of the duplicated 3′ ORFs, was made and their ability to produce infectious virions was analyzed. The data indicate that all eight of the minor structural proteins are required for the efficient production of infectious virions and suggest that SHFV particles are more complex than those of the other known arterivirues.

MATERIALS AND METHODS

Cells and virus

The MA104 cell line was a gift from O. Nianan, Centers for Disease Control and Prevention (Atlanta, GA). These cells were cultured in Minimal Essential Medium (MEM) supplemented with 10% heat-inactivated fetal bovine serum and 10 μg/ml gentamicin at 37°C in a 5% CO_2 atmosphere. SHFV, strain LVR 42-0/6941 (American Type Culture Collection) was sequentially plaque-purified three times and then amplified once on MA104 cells (MOI of 0.01) to produce a stock pool. Virus stocks used for experiments were made by infecting confluent MA104 monolayers with the stock virus at an MOI of 0.2 and harvesting culture fluid at 32 h after infection. Clarified culture fluid (~10^7 PFU/ml) was aliquoted and stored at −80°C.

Generation of overlapping genomic fragments

Genomic RNA was extracted from SHFV-LVR with TRI Reagent (Molecular Research Center, Cincinnati, OH) and 5 overlapping cDNA fragments were synthesized using SuperScript II reverse transcriptase (Invitrogen) and the forward primers listed in Table 1. The fragment junctions were selected based on the locations of *PflMI* recognition sequences (CCANNNN/NTGG). Each fragment cDNA was then amplified by PCR using appropriate set of primers (Table 1). Cycling conditions were 48°C for 30 min, 94°C for 2 min, then 37 cycles of 94°C for 30 s, 55°C for 30 s and 65–72°C for 1 to 5 min followed by a final cycle at 72°C for 7 min to facilitate subsequent TA cloning. A unique SpeI cutting site (for insertion into the pACYC184 vector) and the SP6 promoter were added to the 5′ end of fragment 1 in the forward primer and a 47 nt poly A tail, a unique PvuI site (for linearization) and a unique NotI site (for insertion into the pACYC184 vector) were added to the 3′ end of fragment 5 in the reverse primer (Table 1). Each of the PCR fragments was gel purified and cloned into the pCR-XL-TOPO vector. These plasmids were maintained in TOP10 or INV110 *E.coli* cells (Invitrogen) grown in LB media containing kanamycin (50 mg/ml). Multiple clones of each fragment were generated and sequenced.

Assembly of full-length cDNA clones

Plasmid DNA of each fragment was digested with PflMI alone (fragments 2 and 4) or also with SpeI (fragment 1), RsrII (fragment 3) or NotI and RsrII (fragment 5). The pACYC184 vector was digensted with XbaI and EagI to generate cohesive ends that were compatible with SpeI and NotI, respectively, and then gel purified. The digested SHFV cDNA fragments and vector DNA were simultaneously ligated using a T4 Rapid Ligation kit (Thermo Scientific) and the resulting DNA was used to transform XL10-Gold Kan^R Ultracompetent cells (Stratagene). The cells were grown overnight at 37°C in LB media containing chloramphenicol. The full-length SHFV cDNA clones generated were sequenced to insure that no mutations had occurred during cloning.

In vitro RNA transcription and cell transfection

Full-length cDNA clones were linearized with PvuI, purified on MinElute columns (Qiagen) and used as templates for *in vitro* transcription of capped mRNA using a mMessage mMachine kit (Ambion) according to the manufacturer's protocol. Reactions were incubated at 37°C for 2 h then with DNase for 15 min, followed by LiCl precipitation and an ethanol wash of the pelleted RNA. The final RNA pellet was resuspended in nuclease-free dH_2O. An aliquot of the RNA was denatured with a formamide-based RNA sample buffer (Ambion) and analyzed for size and quality on an RNase-free denaturing gel.

MA104 cells were seeded in a six-well plate and grown overnight to <50% confluency. The cells were washed once with serum-free Opti-MEM (Gibco). The *in vitro* transcribed infectious clone RNA (100 or 500 ng) was mixed with 10 μl DMIRE-C (1, 2-dimyristyloxypropyl-3-dimethyl-hydroxy ethyl ammonium bromide and cholesterol) (Invitrogen) in serum-free Opti-MEM (Gibco) and added to the cells. DMIRE-C without RNA was used as a negative control and DMIRE-C with RNA extracted with TRI Reagent from parental SHFV-LVR virions was used as a positive control. The transfection media was removed after 4 h and 2 ml of fresh media were added to each well. Culture fluid (100 μl) harvested at 120 h was used to infect a fresh MA104 cell monolayer. This procedure was repeated for a total of three or four serial passages. In some cases, the harvested culture fluid was analyzed for viral RNA by qRT-PCR and cell lysates were analyzed for the presence of SHFV nucleocapsid and nsp1β proteins by Western blotting.

454 Sequencing of viral RNA

Viral RNA was isolated from SHFV-LVR and processed as previously described (Donaldson et al., 2010). Briefly, culture fluid was first passed through a 0.45 micron filter to remove large contaminants and then centrifuged at 50,000 × g for 2 hours. The pellets were resuspended in PBS overnight at 4°C and then treated with DNase Turbo, Benzonase, and RNase One for 2 h at 37°C to remove any RNA and DNA that was not protected due to being inside a virion. Virion RNA was then extracted using a Qiagen Viral RNA kit (Qiagen, Valencia, CA) according to manufacturer's instructions. Extracted RNA was reverse transcribed, purified, and amplified as described previously (Donaldson et al., 2010). Briefly, the RNA was reverse transcribed with Superscript III (Life Technologies, Grand Island, NY) according to manufacturer's instructions using random hexamers with a unique barcode. A Klenow reaction was preformed to generate dsDNA from the cDNA. The DNA

was then incubated with phosphatase and exonuclease to remove phosphates and unincorporated primers or single stranded bases, respectively. A total of 10 μl from the Klenow reaction was used as template for random amplification using the unique barcode, without the random hexamer portion, as a primer. The SISPA reactions were gel purified using a QiaQuick Gel Extraction Kit (Qiagen, Valencia, CA). The purified DNA samples were submitted to the University of North Carolina High Throughput Sequencing facility for sequencing using the Roche 454 Life Science FLX Titanium chemistry (454 Life Sciences of Roche, Branford, CT) for the first sequence run. The second sequence run used the Roche 454 Junior platform and chemistry (454 Life Sciences of Roche, Branford, CT).

Sequences derived from Roche 454 sequencing were binned based on the barcode sequence added during the SISPA preparation, and the barcode sequences were trimmed from the reads in each unique bin, representing individual samples. Each sample bin was mapped to the SHFV reference genome (accession no. AF180391.1) using the CLC Genomics Workbench version 5.1 (CLCBio, Aarhus, Denmark; http://www.clcbio.com) using default settings. Consensus sequences were determined for each contig using the 50% majority rule. The 454 sequence bins for each sample were also assembled via *de novo* assembly to determine if the two assembly approaches produced similar results and to identify sequences of unknown identity. The consensus sequences derived by *de novo* assembly were used to query the non-redundant nucleotide database using BLAST within the CLC Genomics Workbench interface. Differences between the reference genome and the genome derived by sequencing were annotated using a multiple sequence alignment generated using the CLC Genomics Workbench.

Construction of minor structural protein knock out mutants

To generate individual mutant infectious clones that did not express one of the eight minor structural proteins, primers were designed to mutate the start codon of one ORF without changing the amino acid sequence of the protein expressed from an overlapping ORF (Table 2). Mutations were introduced using the appropriate primer set (Table 2), infectious clone fragment [Fragment 3 for ORFs 2a′ (ΔGP2), 2b′ (ΔE′) and 3′ (ΔGP3′), Fragment 4 for ORF4′(ΔGP4′) and Fragment 5 for ORF2a (ΔE), 2b (ΔGP2), 3 (ΔGP3) and 4 (ΔGP4)] and a QuikChange Lightning Site-Directed Mutagenesis kit (Agilent Technologies) according to manufacturer's protocol. Briefly, wild type fragment constructs were subjected to PCR using the mutagenic primers, the PCR products were then digested with DpnI to cleave the parental methylated and hemimethylated templates, and the mutant fragment DNAs were transformed into XL10-Gold ultra-competent cells. The mutations and fragment sequences were confirmed by sequencing. One mutant fragment and four wildtype fragments were then digested with the appropriate restriction enzymes and simultaneously assembled, and cloned into the pACYC184 vector as described above and the resulting plasmid was used to *in vitro* transcribe mutant genome RNA for transfection into MA104 cells.

Plaque Assay

Plaque assays were performed on confluent monolayers of MA104 cells in six-well plates. Harvested culture fluids were clarified by centrifugation at 1,000 rpm for 5 min at 4°C, serially diluted 10 fold in growth media and 100 μl of each dilution was added per well.

Each sample was assayed in duplicate. After adsorption for 1 h at room temperature, the inoculum was removed, 2 mls of overlay media [1% SeaKem ME agarose (Bio-Whittaker Molecular Applications) mixed 1:1 with 2 × MEM containing 5% FCS] were added per well and the plates were incubated at 37°C for 72 h. After removal of the agarose plugs, cells were stained with 0.05% crystal violet in 10% ethanol.

Western blot

Culture media was removed from infected MA104 monolayers in 6 well plates and RIPA buffer (1X phosphate-buffered saline, 1% Nonidet P-40, 0.5% sodium deoxycholate, and 0.1% SDS) containing Halt protease inhibitor cocktail (Thermo Scientific) was added to lyse the cells. Lysate proteins were separated by SDS-PAGE and then transferred to a nitrocellulose membrane by electrophoresis. Membranes were blocked with 1X Tris-buffered saline (TBS), pH 8.0, containing 5% non-fat dry milk and 0.1% Tween 20 before incubation with a polyclonal primary antibody specific for an SHFV nucleocapsid peptide (NETHYVFAEPGDLRC), an SHFV nsp1β peptide (FAQKVITAFPEGVLC) or actin (C-11; Santa Cruz Biotechnology, Santa Cruz, CA) in the presence of blocking buffer. Blots were washed with 1X TBS and incubated with secondary antibody (horseradish peroxidase-conjugated anti-rabbit or anti-mouse; Santa Cruz Biotechnology) and then processed for chemiluminescence using a Super-Signal West Pico detection kit (Pierce, Rockford, IL) according to manufacturer's protocol.

Digoxigenin (DIG)-labeled SHFV 5′ leader probe

PCR primers were designed to amplify a region in the 5′-leader (genome nts 7 to 200) for use as a template for making a 5′-leader probe (Table 3). The reverse primer included a T7 promoter. The PCR product generated was validated by sequencing and then *in vitro* transcribed with T7 RNA polymerase in the presence of DIG-labeled UTP using a DIG Northern Starter Kit (Roche) according to the manufacturer's protocol. The concentration of the DIG-labeled probe was determined by a dot-blot assay using dilutions of a DIG-labeled human actin RNA probe of known concentration as a reference (Roche). Briefly, 1 μl of each dilution was spotted onto an Amersham Hybond-N^+ membrane (GE Healthcare) and then UV-crosslinked. The membrane was blocked with DIG blocking solution (Roche), incubated with anti-DIG antibody (1:10,000 dilution, Roche) and then with CDP-Star (Roche). The signal was detected with an LAS4000 mini Luminescent Image Analyzer (GE Healthcare). Spot intensities were determined using Multi Gauge V2.3 software.

Northern Blot hybridization

MA-104 cell monolayers in 6 well plates were either mock infected or infected with SHFV infectious clone virus at a MOI of 1. At different times after infection, total cell RNA was extracted with TRI reagent (Molecular Research Center, Inc.). One μg of RNA was mixed with NorthernMax formaldehyde loading dye (Ambion), denatured at 80°C for 10 min and then separated on a 1% formaldehyde agarose gel for 2.5 h at 100V. RNA markers (Millennium Markers-Formamide, Ambion) were run on one lane of the gel. RNA was transferred overnight by capillary action onto an Amersham Hybond-N^+ membrane (GE Healthcare) and the RNA was then UV-crosslinked to the membrane. The lane containing

the RNA standards was cut from the membrane and stained with methylene blue. The rest of the membrane was pre-hybridized with DIG Easy Hyb buffer (Roche) at 68°C for 30 min and then hybridized with 100 ng/mL of a DIG-labeled, denatured RNA probe at 68°C overnight. The hybridized membrane was washed first with low stringency buffer (2X SSC + 0.1% SDS) at room temperature, then with high stringency buffer (0.1X SSC + 0.1% SDS) at 68°C followed by blocking with DIG blocking solution (Roche). To detect the RNA bands, membranes were incubated with anti-DIG antibody (1:10,000 dilution) (Roche), developed with CDP-Star (Roche) and imaged with an LAS4000 mini Luminescent Image Analyzer (GE Healthcare).

Analysis of extracellular viral RNA by quantitative real-time RT-PCR

RNA in 200 μl of culture fluid harvested from infectious clone transfected MA104 monolayers was extracted with TRI Reagent. Reaction mixtures contained extracted RNA, the primer pair (1 μM) and probe (0.2 μM) in a final volume of 10 μl. Primer/probe sequences targeted either the nucleocapsid (forward primer 5'-tcccacctcagcacacatca-3', TaqMan probe 5′-6FAMaacagctgctgatcaggtMGBNFQ-3′ and reverse primer 5′-ccgcctccgttgtcgtagt-3′) or helicase (nsp9) (forward primer 5′-cgtacacccgccgtctgct-3′, TaqMan probe 5′-6FAMttgacgttctcacaaaggMGBNFQ-3′, and reverse primer 5′-cggcaagtggcatccaa-3′) regions. Quantitative real time RT-PCR was performed and the data were analyzed as previously described (Scherbik et al., 2006). Extracellular SHFV genomic RNA was quantified using a standard curve generated with serial dilutions of a known concentration of SHFV RNA that had been *in vitro* transcribed with a MAXIscript SP6 transcription kit (Ambion) from either the nucleocapsid or nsp9 gene region of the SHFVic cDNA, digested with DNase, extracted with phenol-chloroform, precipitated with ethanol and then quantified by UV spectrophotometry.

RESULTS

Construction of a full-length cDNA infectious clone of SHFV-LVR

A full-length cDNA clone of the SHFV, strain LVR, genome was constructed using a previously described strategy (Fang et al., 2006b; Nielson et al., 2003; Yount et al., 2000; Yount et al., 2002). Five overlapping cDNA fragments covering the genome were amplified from SHFV RNA by RT-PCR as described in Materials and Methods (Fig. 1B and C). A few nts in each fragment differed from the Genbank SHFV consensus sequence (Accession number AF180391.1) and initially each of these nts was corrected by site-directed mutagenesis of the appropriate fragment clone. The corrected individual fragment clones were then cut with PflMI, simultaneously ligated and cloned into pACYC184. The complete cDNAs in three clones were sequenced and no unexpected mutations were found. MA104 cells transfected with either 100 or 500 ng of *in vitro* transcribed SHFV RNA were observed daily for the development of cytopathic effect (CPE). At 120 h after transfection, cells were lysed and the lysates analyzed for SHFV nucleocapsid and nsp1β proteins by Western blotting. The transfected cells did not show any obvious CPE and viral proteins were not detected in cell lysates through 120 h (data not shown). The harvested culture fluid was serially passaged four times in an attempt to recover virus but neither CPE nor intracellular viral protein was detected after any of these passages (data not shown).

Because the Genbank consensus sequence (GenBank Assession number AF180391.1) of SHFV LVR was obtained by older sequencing methods from shot gun clones and it was likely that this sequence contained deleterious errors. Viral RNA extracted from parental SHFV LVR was subjected to 454 sequencing as described in Materials and Methods. In addition, each of the fragment clones was reamplified from SHFV LVR RNA by RT-PCR and sequenced. The same 18 nt differences compared with the previous GenBank consensus sequence were detected by both 454 genomic sequencing and individual fragment sequencing (Table 4). The GenBank sequence was updated based on the 454 sequencing data (GenBank Assession number XXX). (The updates have been submitted and the ID will be added after it is received). The reamplified fragment clones were then used to construct a new full-length clones (SHFVic). The sequences of three full length clones were confirmed. Viral RNA was *in vitro* transcribed from linearized plasmid RNA and analyzed on an RNase-free denaturing agarose gel (Fig. 1D). Six RNA bands with sizes of about 15, 13, 12, 7, 4 and 3 kb were consistently detected. The 15 kb band was appropriately sized to represent the full-length viral genome RNA. The shorter products were likely the result of premature termination or aberrant transcription. MA104 cells transfected with either 100 or 500 ng of *in vitro* transcribed SHFVic RNA showed CPE by 72 h after transfection and Western blot analysis detected nsp1β in lysates from cells transfected with either concentration of viral RNA at 72 h after transfection (Fig. 2A). The higher amount of viral protein detected after transfection of 100 ng of RNA suggested the possibility that increased amounts of the shorter RNAs negatively affected the efficiency of viral replication. To confirm that extracellular infectious virus was produced, 100 μl of undiluted culture fluid from the transfected cells was passaged onto fresh MA104 cells. These cells showed CPE starting at 24 h after infection and Western blot analysis detected intracellular nsp1β protein in cell lysates harvested at 72 h (Fig. 2A).

To compare the replication kinetics of the infectious clone virus and the parental virus, MA104 cells were infected with either first passage infectious clone virus or with SHFV-LVR parental virus at an MOI of 1 and viral yields were quantified by plaque assay on MA104 cells at various times after infection (Fig. 2B). The replication kinetics of the parental virus and the infectious clone virus were similar and both cultures produced peak titers of ~10^6 PFU/ml by 72 h after infection. The kinetics of intracellular viral protein synthesis were assessed by Western blotting of lysates from replicate cultures. Similar kinetics of production and levels of intracellular nsp1β and nucleocapsid were detected by Western blotting in parental and SHFVic virus infected cell lysates (Fig. 2C). The data indicate that the replication efficiency of virus derived from the infectious clone is comparable to that of the parental LVR virus.

Analysis of SHFV sg mRNA production in infected cells

EAV produces six sg mRNAs in infected MA104 cells (Snijder and Meulenberg, 1998; van Berlo et al., 1982) and sg mRNA 2 was subsequently shown to be bicistronic expressing both GP2 and E (Snijder et al., 1999). Because the sequence obtained for the 3′ end of the SHFV genome indicated the presence of a duplicated set of minor structural ORFs (Godeny et al., 1998), 9 sg SHFV mRNAs were predicted. However, evidence for only 8 was obtained due to the lack of detection of a PCR band containing a sg mRNA junction

sequence for the second minor GP ORF (Godeny et al., 1998). The existence of an ORF for the E′ protein overlapping the first minor GP ORF was not known at that time. The first and second SHFV minor GP ORFs were therefore named ORF2a and ORF2b because it was assumed that these GPs were expressed from a bicistronic sg mRNA (Godeny et al., 1998).

The sg mRNAs produced by MA104 cells infected with SHFVic virus were analyzed by Northern blotting using a DIG-labeled 5′ leader probe (Fig. 3A). The 15.7 kb genome and nine sg mRNA bands with sizes of 5.0, 4.4, 4.0, 3.5, 2.8, 2.6, 1.9, 1.2 and 0.6 kb were detected starting at 8 h after infection. The detection of 5.0 and 4.4 kb sg mRNAs suggested that separate sg mRNAs are expressed for ORF2b. To confirm that separate sg mRNAs were expressed for ORF2a and ORF2b, a set of RT-PCR primers (Table 3) was designed that were predicted to amplify the junction regions of both the ORF2a (now ORF2′) and ORF2b (now ORF3′) sg mRNAs (Fig. 3B, top). The RT-PCR products generated from total cell RNA isolated from MA104 cells infected with SHFVic virus for 24 h were separated on an agarose gel and visualized by ethidium bromide staining. A strong band of ~1000 bp and a weaker PCR band of ~500 bp were detected (Fig. 3B, bottom). These bands were excised and the PCR products present in each band were TA cloned and sequenced. The predominant junction sequence identified in the ~1000 kb band was identical to the one previously reported for sg mRNA 2a (data not shown) (Godeny et al., 1998). The junction sequence found in the weaker ~500 kb band is shown in Fig. 3C. Based on the detection of the 4.4 kb sg mRNA and current knowledge that the sg mRNA of the former ORF2a is bicistronic because it contains an E protein ORF, the SHFV ORF formerly named ORF2b was renamed ORF3′ (Fig. 3A). To facilitate comparison of the structural ORFs among the arteriviruses, the duplicated sets of SHFV minor structural ORFS and proteins were renamed ORF2a′ (GP2′), ORF2b′ (E′), ORF3′ (GP3′), ORF4′ (GP4′) and ORF2a (E), ORF2b (GP2), ORF3 (GP3), ORF4 (GP4) (Fig. 1A) (Snijder and Kikkert, 2013).

The relative intensities of the individual sg mRNA bands differed with sg mRNA 2′, 2, 5, 5, and 7 being the most abundant. Previous Northern blot analyses of the SHFV sg mRNAs done before it was known that the SHFV genome encoded additional 3′ ORFs detected only these five strong sg mRNA bands (Godeny et al., 1995; Zeng et al., 1995). Interestingly, the relative abundance of the sg mRNAs for the orthologs in the duplicated sets of SHFV 3′ ORFs were similar with sg mRNAs 2′ and 2 being abundantly expressed while sg mRNAs 3′, 3, 4′ and 4 were expressed at low levels.

Analysis of the functional importance of the individual minor structural proteins

The SHFV genome is predicted to encode two sets of minor structural proteins while the LDV, EAV and PRRSV genomes encode a single set (Godeny et al., 1998). Recent data indicate that all four of the minor structural proteins of EAV and PRRSV are required for viral attachment/entry (Snijder and Kikkert, 2013; Tian et al., 2012). To analyze the functions of the individual SHFV minor structural proteins, the translation start codon for each of the 8 minor structural proteins was individually mutated in the appropriate genomic fragment clone without altering the amino acid coded in an overlapping ORF (Table 2). Three full-length clones were then assembled for each of the minor structural protein knock-out mutants. I*n vitro* transcribed viral RNA (100 ng) for each of the 3 clones was separately

transfected into MA104 cells. RNA from a replication deficient polymerase mutant (conserved SDD changed to SAA) was also constructed and used as a negative control. Wildtype SHFVic RNA was used as a positive control. Transfected cells were observed daily for CPE through 120 h after tranfection. Cells transfected with viral RNA transcribed from each of the minor structural protein mutant clones showed no CPE by 120 h after transfection with the exception of one of the three replicate ΔGP4′ viral RNAs which produced CPE at 72 h after transfection comparable to that observed after transfection with the wild type SHFVic RNA. Only the other two ΔGP4′ mutants were further analyzed. Cells transfected with RNA transcribed from the SAA mutant clone also showed no CPE. Culture fluid harvested at 120 h after transfection of the mutant RNAs was next passaged onto fresh MA104 cells and the cells were observed daily for CPE. No CPE was observed by 120 h after the first passage or during an additional four serial blind passages on MA104 cells.

To determine whether extracellular viral particles were produced by any of the mutant RNA transfected cells, RNA was extracted from culture fluids harvested at various times after transfection and the amount of viral RNA present was quantified by qRT-PCR. Data was obtained for two independent clones for each mutant and all samples were analyzed independently using primers and probe targeting either the nucleocapsid and or nsp9 regions of the genome RNA. Because very similar data were obtained with both primer/probe sets, only the data obtained with the nucleocapsid primers/probe set are shown. Transfection of wildtype SHFVic RNA resulted in a large increase in extracellular viral RNA starting at 96 h after transfection with viral RNA levels continuing to increase through 120 h. In contrast, transfection of SAA mutant RNA did not result in an increase in extracellular viral RNA above background levels at any time tested. Transfection of ΔGP2′ or ΔGP3′ mutant RNA did not result in an increase in extracellular viral RNA above background levels at any of the times analyzed (Fig. 4A and B). In contrast, an increase in extracellular viral RNA was detected beginning at 24 h after transfection of ΔGP4′, ΔGP2 or ΔGP3 mutant RNA indicating that extracellular progeny particles were produced by each of these mutants (Fig. 4C–E). A sustained low level of extracellular viral RNA would be expected if only a single cycle infection occurred and virus particles were produced from the few cells transfected with a replication competent, full length copy of *in vitro* transcribed mutant viral RNA. Interestingly, between 24 and 72 h, the relative amounts of extracellular viral RNA were higher in culture fluids from cells transfected with ΔGP4′, ΔGP2, or ΔGP3 mutant RNA than in culture fluids from cultures transfected with wildtype RNA. This observation is consistent with the accumulation of non-infectious virus particles in the mutant RNA transfected culture fluids. Infectious wildtype virus would not be expected to accumulate initially due its ability to efficiently attach to and entry cells. Cells transfected with ΔGP4 mutant RNA produced increased levels of extracellular viral RNA by 24 h after transfection than cells transfected with the wildtype RNA suggesting that the particles produced by this mutant RNA were also not infectious (Fig. 4F). However, the level of ΔGP4 extracellular viral RNA decreased by 48 h suggesting a possible role for GP4 in virion stability. For each of the mutants, intracellular nsp1β levels in cell lysates collected at 120 h after transfection and at 120 h after a single blind passage were analyzed by Western blotting. Nsp1β was not detected in cells transfected with any of the mutant RNAs or in any of the passage 1 cells (Fig. 4G). The lack of detection of intracellular viral protein is consistent with a lack of virus

spread and the levels of viral protein in the few productively transfected cells being too low to detect by Western blotting. Mutant infectious clones were next made that had the AUGs of both GP2′ and GP2, both GP3′ and GP3, or both GP4′ and GP4 mutated. No CPE was observed by 120 h after transfection with any of these double mutant RNAs or during four subsequent serial blind passages of the culture fluids. No extracellular viral RNA was detected in culture fluids harvested from cells transfected with any of the double mutant RNAs (Fig. 4H–J) and no detectable intracellular nsp1β protein was detected after transfection or passage (Fig. 4K).

No CPE was observed in cells transfected with ΔE′ or ΔE mutant viral RNA or during five subsequent serial blind passages of culture fluid. No significant increase extracellular viral RNA above background levels was detected in culture fluids from cells transfected with either ΔE′ or ΔE mutant RNA (Fig. 5A and B). No intracellular nsp1β protein was detected at 120 h after transfection or at 120 h after passage 1 (Fig. 5C). The results suggest that both the SHFV E′ and E proteins play a role in virus particle production.

DISCUSSION

The EAV, PRRSV and LDV genomes encode four minor structural proteins, GP2, E, GP3 and GP4. The SHFV genome is unique in having a second set of the minor structural protein ORFs that are proposed to have been acquired by copy choice recombination between two SHFV genomes (Smith et al., 1997). It had also been suggested that the minor structural protein gene sequence duplication might be a laboratory artifact unique to the SHFV LVR strain (Tauraso et al., 1968). However, the additional set of SHFV 3′ ORFs was reported to be present in SHFV isolates recently obtained from naturally infected Red colobus and Red-tailed guenon (Lauck et al., 2011; Lauck et al., 2013) and also from persistently infected baboons (Vatter and Brinton, unpublished data).

Infectious clones for multiple strains of EAV and PRRSV have been constructed (Balasuriya et al., 2007; Fang et al., 2006a; Lv et al., 2008; Meulenberg et al., 1998; Nielson et al., 2003; van Dinten et al., 1997) and these infectious clones have been used to investigate viral replication as well as the induction and counteraction of host immune responses. SHFVic is the first SHFV infectious clone and the longest arterivirus RNA genome cDNA to date to be stably maintained within a single plasmid. The successful generation of SHFVic provides a unique tool for analyzing the functions of individual virus proteins and for identifying SHFV virulence determinants for macaques. In the present study, SHFVic was used for a reverse genetics analysis of the effects of separately “knocking out” the expression of each of the eight SHFV minor structural proteins in the duplicated sets.

Data previously obtained with EAV and PRRSV indicate that virus particles containing genome RNA are still produced when only the major structural proteins, N, M and GP5, are expressed (Wieringa et al., 2004a; Wissink et al., 2005; Zevenhoven-Dobbe et al., 2004). EAV GP2 and GP4 form heterodimers through intermolecular cysteine bridges (Wieringa et al., 2003a). After virion release, a post-assembly maturation occurs resulting in EAV GP3 becoming disulfide bonded to GP2-GP4 heterodimers forming GP2-GP3-GP4 heterotrimers (Wieringa et al., 2003b; Wieringa et al., 2004b). GP3 of Type 2 PRRSV strains is required

for formation of the GP2/GP4 heterodimer (Dea et al., 2000). The PRRSV GP4 is required for the interaction of GP2-GP3-GP4 heterotrimers with the major glycoprotein GP5 (Das et al., 2010). The C-terminal domain of PRRSV GP4 functions as a GPI anchor and expressed GP4 colocalizes with CD163 in lipid rafts on the plasma membrane (Du et al., 2012). The E protein appears to be associated with the GP2-GP3-GP4 heterotrimer on the surface of virions (Wieringa et al., 2004a) and to function as an ion channel during virus entry (Lee and Yoo, 2006) and knockout of the expression of GP2, GP3, GP4 or E blocked the incorporation of the minor GP heterotrimer into virion particles (Wieringa et al., 2004a; Wieringa et al., 2003b; Wissink et al., 2005; Zevenhoven-Dobbe et al., 2004). Based on sequence homology between SHFV minor structural protein orthologs and the respective homologs of other arteriviruses, it was previously suggested that the two sets of SHFV minor structural glycoproteins might be functionally redundant (Godeny et al., 1998). However, in the present study different phenotypes were detected for the ΔGP2′ and ΔGP2 mutant RNAs (Fig. 4A and D) and also for the ΔGP3′ and ΔGP3 mutant RNAs (Fig. 4B and E) and the ΔGP4′ and ΔGP4 RNAs (Fig. 4C an F). No extracellular viral RNA was detected when either GP2′ or GP3′ expression was knocked out indicating that these two proteins are required for virion assembly, release and/or stability. However, the possibility that one or both of these proteins may also be involved in virion infectivity cannot be ruled out. Sustained low levels of extracellular viral RNA were produced when GP2, GP3 or GP4′ expression was knocked out but no amplification of the viral RNA at later times was detected indicating that non-infectious virus particles were produced. It is possible that these three minor SHFV GP proteins form a complex that functions similarly to the GP2-GP3-GP4 heterotrimer of other arteriviruses. Although both the ΔGP4′ and ΔGP4 mutant RNAs produced non-infectious virus particles, the production of these particles was not sustained when GP4 was not expressed suggesting that GP4 may also play a role in virion particle stability. The finding that each of the SHFV minor GPs was required for the production of infectious virions as well as the observation of different phenotypes for the orthologs of the two sets of SHFV minor GPs indicate that the duplicated sets of SHFV minor structural proteins are not functionally redundant. The LDV, EAV and PRRSV E proteins are each translated from bicistronic sg mRNA 2. However, the location of the start codon of the E protein ORF relative to that of the GP2 protein ORF in sg mRNA 2 differs among these genomes. GP2 translation is initiated from the 5′ AUG (ORF2a) and E translation is initiated at a downstream AUG (ORF2b) in the PRRSV sg mRNA 2, whereas in the sg mRNA 2 of LDV and EAV, the E protein is initiated from the 5′ most AUG (ORF2a) and GP2 is initiated from a downstream AUG (ORF2b). In the SHFV sg mRNA 2′, ORF2a′ (GP2′) is upstream of ORF2b′ (E′) similar to the order in PRRSV sg mRNA 2. In contrast, in the SHFV sg mRNA 2, ORF2b (E) is upstream of ORF2a (GP2) similar to the EAV and LDV gene order (see Fig. 1A). The E protein sequences of EAV, PRRSV and LDV contain a conserved N-terminal myristoylation site (Thaa et al., 2009). Inhibition of myristoylation during EAV replication decreased virus infectivity and plaque size but not the amount of extracellular virus suggesting that myristoylation of E is not required for virion budding or release but facilitates infectivity (Thaa et al., 2009). The SHFV E protein sequence contains the conserved N-terminal myristoylation site but the SHFV E′ protein sequence does not. Extracellular viral RNA was not produced by cells transfected with either ΔE′ or ΔE mutant RNA. These data suggest that both SHFV E′ and E also play a role in virion production/

stability. Although previous studies with EAV showed that knocking out of GP2, GP3, GP4 or E expression blocked the incorporation of the minor GP heterotrimer into virion particles, a role for E in virion assembly or stability has not been reported (Wieringa et al., 2004a; Wieringa et al., 2003b; Wissink et al., 2005; Zevenhoven-Dobbe et al., 2004). Additional studies are required to determine whether the SHFV E and/or E′ proteins have functions during virus attachment and/or entry. The data obtained indicate that each of the proteins in the duplicated sets of SHFV minor structural proteins are required for the production of infectious virions. Among RNA viruses, SHFV particles appear to contain the largest number of envelop proteins.

Acknowledgments

This work was supported by a Public Health Service research grant AI073824 to M.A.B from the National Institute of Allergy and Infectious Diseases, National Institutes of Health. H.A.V. and H.D. were supported by a Molecular Basis of Disease Fellowship from Georgia State University. The high performance sequencing using the 454 platform was funded in part by an ARRA grant through SERCEB no. U54-AI057157PI awarded to E.F.D. We thank Mausumi Basu for assistance with preparation of the figures.

REFERENCES

Allen AM, Palmer AE, Tauraso NM, Shelokov A. Simian hemorrhagic fever. II. Studies in pathology. The American journal of tropical medicine and hygiene. 1968; 17:413–421. [PubMed: 4968100]

Balasuriya UB, Snijder EJ, Heidner HW, Zhang J, Zevenhoven-Dobbe JC, Boone JD, McCollum WH, Timoney PJ, MacLachlan NJ. Development and characterization of an infectious cDNA clone of the virulent Bucyrus strain of Equine arteritis virus. J Gen Virol. 2007; 88:918–924. [PubMed: 17325365]

Beerens N, Selisko B, Ricagno S, Imbert I, van der Zanden L, Snijder EJ, Canard B. De novo initiation of RNA synthesis by arterivirus RNA-dependent RNA polymerase. J Virol. 2007; 81:8384–8395. [PubMed: 17537850]

Bray M. Pathogenesis of viral hemorrhagic fever. Current opinion in immunology. 2005; 17:399–403. [PubMed: 15955687]

Calvert JG, Slade DE, Shields SL, Jolie R, Mannan RM, Ankenbauer RG, Welch SK. CD163 expression confers susceptibility to porcine reproductive and respiratory syndrome viruses. J Virol. 2007; 81:7371–7379. [PubMed: 17494075]

Dalgard DW, Hardy RJ, Pearson SL, Pucak GJ, Quander RV, Zack PM, Peters CJ, Jahrling PB. Combined simian hemorrhagic fever and Ebola virus infection in cynomolgus monkeys. Laboratory animal science. 1992; 42:152–157. [PubMed: 1318446]

Das PB, Dinh PX, Ansari IH, de Lima M, Osorio FA, Pattnaik AK. The minor envelope glycoproteins GP2a and GP4 of porcine reproductive and respiratory syndrome virus interact with the receptor CD163. J Virol. 2010; 84:1731–1740. [PubMed: 19939927]

Dea S, Gagnon CA, Mardassi H, Pirzadeh B, Rogan D. Current knowledge on the structural proteins of porcine reproductive and respiratory syndrome (PRRS) virus: comparison of the North American and European isolates. Arch Virol. 2000; 145:659–688. [PubMed: 10893147]

Delputte PL, Van Breedam W, Delrue I, Oetke C, Crocker PR, Nauwynck HJ. Porcine arterivirus attachment to the macrophage-specific receptor sialoadhesin is dependent on the sialic acid-binding activity of the N-terminal immunoglobulin domain of sialoadhesin. J Virol. 2007; 81:9546–9550. [PubMed: 17567703]

Delputte PL, Vanderheijden N, Nauwynck HJ, Pensaert MB. Involvement of the Matrix Protein in Attachment of Porcine Reproductive and Respiratory Syndrome Virus to a Heparinlike Receptor on Porcine Alveolar Macrophages. J Virol. 2002; 76:4312–4320. [PubMed: 11932397]

Donaldson EF, Haskew AN, Gates JE, Huynh J, Moore CJ, Frieman MB. Metagenomic analysis of the viromes of three North American bat species: viral diversity among different bat species that share a common habitat. J Virol. 2010; 84:13004–13018. [PubMed: 20926577]

Du Y, Pattnaik AK, Song C, Yoo D, Li G. Glycosyl-phosphatidylinositol (GPI)-anchored membrane association of the porcine reproductive and respiratory syndrome virus GP4 glycoprotein and its co-localization with CD163 in lipid rafts. Virology. 2012; 424:18–32. [PubMed: 22222209]

Dunowska M, Biggs PJ, Zheng T, Perrott MR. Identification of a novel nidovirus associated with a neurological disease of the Australian brushtail possum (Trichosurus vulpecula). Vet Microbiol. 2012; 156:418–424. [PubMed: 22153843]

Fang Y, Faaberg KS, Rowland RR, Christopher-Hennings J, Pattnaik AK, Osorio F, Nelson EA. Construction of a full-length cDNA infectious clone of a European-like Type 1 PRRSV isolated in the U.S. Advances in experimental medicine and biology. 2006a; 581:605–608.

Fang Y, Rowland RRR, Roof M, Lunney JK, Christopher-Hennings J, Nelson EA. A Full-Length cDNA Infectious Clone of North American Type 1 Porcine Reproductive and Respiratory Syndrome Virus: Expression of Green Fluorescent Protein in the Nsp2 Region. J Virol. 2006b; 80:11447–11455. [PubMed: 16971421]

Firth AE, Zevenhoven-Dobbe JC, Wills NM, Go YY, Balasuriya UB, Atkins JF, Snijder EJ, Posthuma CC. Discovery of a small arterivirus gene that overlaps the GP5 coding sequence and is important for virus production. J Gen Virol. 2011; 92:1097–1106. [PubMed: 21307223]

Godeny EK, deVries AAF, Wang XC, Smith SL, deGroot RJ. Indentification of the Leader-Body Junctions for the Viral Subgenomic mRNAs and Organization of the Simian Hemorrhagic Fever Virus Genome: Evidence for Gene Duplication during Arterivirus Evolution. J Virol. 1998; 72:862–867. [PubMed: 9420301]

Godeny EK, Zeng L, Smith SL, Brinton MA. Molecular characterization of the 3' terminus of the simian hemorrhagic fever virus genome. J Virol. 1995; 69:2679–2683. [PubMed: 7884922]

Gravell, M.; London, WT.; Leon, ME.; Palmer, AE.; Hamilton, RS. Differences among isolates of simian hemorrhagic fever (SHF) virus. Proceedings of the Society for Experimental Biology and Medicine; New York, N.Y: Society for Experimental Biology and Medicine; 1986. p. 112-119.

Johnson CR, Griggs TF, Gnanandarajah J, Murtaugh MP. Novel structural protein in porcine reproductive and respiratory syndrome virus encoded by an alternative ORF5 present in all arteriviruses. J Gen Virol. 2011; 92:1107–1116. [PubMed: 21307222]

Lauck M, Hyeroba D, Tumukunde A, Weny G, Lank SM, Chapman CA, O'Connor DH, Friedrich TC, Goldberg TL. Novel, divergent simian hemorrhagic fever viruses in a wild Ugandan red colobus monkey discovered using direct pyrosequencing. PLoS One. 2011; 6:e19056. [PubMed: 21544192]

Lauck M, Sibley SD, Hyeroba D, Tumukunde A, Weny G, Chapman CA, Ting N, Switzer WM, Kuhn JH, Friedrich TC, O'Connor DH, Goldberg TL. Exceptional simian hemorrhagic fever virus diversity in a wild African primate community. J Virol. 2013; 87:688–691. [PubMed: 23077302]

Lee C, Yoo D. The small envelope protein of porcine reproductive and respiratory syndrome virus possesses ion channel protein-like properties. Virology. 2006; 355:30–43. [PubMed: 16904148]

London WT. Epizootiology, transmission and approach to prevention of fatal simian haemorrhagic fever in rhesus monkeys. Nature. 1977; 268:344–345. [PubMed: 18679]

Lv J, Zhang J, Sun Z, Liu W, Yuan S. An infectious cDNA clone of a highly pathogenic porcine reproductive and respiratory syndrome virus variant associated with porcine high fever syndrome. J Gen Virol. 2008; 89:2075–2079. [PubMed: 18753215]

Meulenberg JJM, Bos-deRuijter JNA, vandeGraaf R, Wensvoort G, Moormann RJM. Infectious Transcripts from Cloned Genome-Length cDNA of Porcine Reproductive and Respiratory Syndrome Virus. J Virol. 1998; 72:380–387. [PubMed: 9420236]

Nielson HS, Liu G, Nielsen J, Oleksiewicz MB, Botner A, Storgaard T, Faaberg KS. Generation of an Infectious Clone of VR-2332, a Highly Virulent North American-Type Isolate of Porcine Reproductive and Respiratory Syndrome Virus. J Virol. 2003; 77:3702–3711. [PubMed: 12610145]

Palmer AE, Allen AM, Tauraso NM, Shelokov A. Simian hemorrhagic fever. I. Clinical and epizootiologic aspects of an outbreak among quarantined monkeys. The American journal of tropical medicine and hygiene. 1968; 17:404–412. [PubMed: 4968099]

Scherbik SV, Paranjape JM, Stockman BM, Silverman RH, Brinton MA. RNase L plays a role in the antiviral response to West Nile virus. J Virol. 2006; 80:2987–2999. [PubMed: 16501108]

Smith SL, Wang XC, Godney EK. Sequence of the 3' end of the simian hemorrhagic fever virus genome. Gene. 1997; 191:205–210. [PubMed: 9218721]

Snijder, EJ.; Kikkert, M. Arteriviruses. In: Knipe, DM.; Howley, PM., editors. Fields Virology. 6th ed.. Lippincott, Williams and Wilkins; Philadelphia, PA: 2013. p. 859-879.

Snijder EJ, Meulenberg JJM. The molecular biology of arterivirus. J Gen Virol. 1998; 79:961–979. [PubMed: 9603311]

Snijder EJ, van Tol H, Pedersen KW, Raamsman MJ, de Vries AA. Identification of a novel structural protein of arteriviruses. J Virol. 1999; 73:6335–6345. [PubMed: 10400725]

Sun L, Li Y, Liu R, Wang X, Gao F, Lin T, Huang T, Yao H, Tong G, Fan H, Wei Z, Yuan S. Porcine reproductive and respiratory syndrome virus ORF5a protein is essential for virus viability. Virus Res. 2013; 171:178–185. [PubMed: 23219923]

Tauraso NM, Shelokov A, Palmer AE, Allen AM. Simian hemorrhagic fever. 3. Isolation and characterization of a viral agent. The American journal of tropical medicine and hygiene. 1968; 17:422–431. [PubMed: 4297405]

Thaa B, Kabatek A, Zevenhoven-Dobbe JC, Snijder EJ, Herrmann A, Veit M. Myristoylation of the arterivirus E protein: the fatty acid modification is not essential for membrane association but contributes significantly to virus infectivity. J Gen Virol. 2009; 90:2704–2712. [PubMed: 19656967]

Tian D, Wei Z, Zevenhoven-Dobbe JC, Liu R, Tong G, Snijder EJ, Yuan S. Arterivirus minor envelope proteins are a major determinant of viral tropism in cell culture. J Virol. 2012; 86:3701–3712. [PubMed: 22258262]

van Berlo MF, Horzinek MC, van der Zeijst BA. Equine arteritis virus-infected cells contain six polyadenylated virus-specific RNAs. Virology. 1982; 118:345–352. [PubMed: 6283728]

Van Breedam W, Delputte PL, Van Gorp H, Misinzo G, Vanderheijden N, Duan X, Nauwynck HJ. Porcine reproductive and respiratory syndrome virus entry into the porcine macrophage. J Gen Virol. 2010; 91:1659–1667. [PubMed: 20410315]

van Dinten LC, den Boon JA, Wassenaar AL, Spaan WJ, Snijder EJ. An infectious arterivirus cDNA clone: identification of a replicase point mutation that abolishes discontinuous mRNA transcription. Proceedings of the National Academy of Sciences of the United States of America. 1997; 94:991–996. [PubMed: 9023370]

Van Gorp H, Van Breedam W, Delputte PL, Nauwynck HJ. Sialoadhesin and CD163 join forces during entry of the porcine reproductive and respiratory syndrome virus. J Gen Virol. 2008; 89:2943–2953. [PubMed: 19008379]

Welch SK, Calvert JG. A brief review of CD163 and its role in PRRSV infection. Virus Res. 2010; 154:98–103. [PubMed: 20655964]

Wieringa R, de Vries AA, van der Meulen J, Godeke GJ, Onderwater JJ, van Tol H, Koerten HK, Mommaas AM, Snijder EJ, Rottier PJ. Structural protein requirements in equine arteritis virus assembly. J Virol. 2004a; 78:13019–13027. [PubMed: 15542653]

Wieringa R, deVries AAF, Post SM, Rottier PJM. Intra- and Intermolecular Disulfide Bonds of the GP2b Glycoprotein of Equine Arteritis Virus: Relevance for Virus Assembly and Infectivity. J Virol. 2003a; 77:12996–13004. [PubMed: 14645556]

Wieringa R, deVries AAF, Rottier PJM. Formation of Disulfide-Linked Complexes between the Three Minor Envelope Glycoproteins (GP2b, GP3, and GP4) of Equine Arteritis Virus. J Virol. 2003b; 77:6216–6226. [PubMed: 12743278]

Wieringa R, deVries AAF, vanderMeulen J, Godeke G-J, Onderwater JJM, vanTol H, Koerten HK, Mommaas AM, Snijder EJ, Rottier PJM. Structural Protein Requirements in Equne Arteritis Virus Assembly. J Virol. 2004b; 78:13019–13027. [PubMed: 15542653]

Wissink EH, Kroese MV, van Wijk HA, Rijsewijk FA, Meulenberg JJ, Rottier PJ. Envelope protein requirements for the assembly of infectious virions of porcine reproductive and respiratory syndrome virus. J Virol. 2005; 79:12495–12506. [PubMed: 16160177]

Yount B, Curtis KM, Baric RS. Strategy for Systematic Assembly of Large RNA and DNA Genomes: Transmissible Gastroenteritis Virus Model. J Virol. 2000; 74:10600–10611. [PubMed: 11044104]

Yount B, Denison MR, Weiss SR, Baric RS. Systematic Assembly of a Full-Length Infectious cDNA of Mouse Hepatitis Virus Strain A59. J Virol. 2002; 76:11065–11078. [PubMed: 12368349]

Zeng L, Godney EK, Methven SL, Brinton MA. Analysis of Simian Hemorrhagic Fever Virus (SHFV) Subgenomic RNAs, Junction Sequences, and 5' Leader. Virology. 1995; 207:543–548. [PubMed: 7886957]

Zevenhoven-Dobbe JC, Greve S, van Tol H, Spaan WJ, Snijder EJ. Rescue of disabled infectious single-cycle (DISC) equine arteritis virus by using complementing cell lines that express minor structural glycoproteins. J Gen Virol. 2004; 85:3709–3714. [PubMed: 15557244]

HIGHLIGHTS

- A stable infectious clone of 15.7 kb SHFV cDNA was generated.
- The functional redundancy of SHFV minor structural ortholog proteins was analyzed.
- Both sets of minor structural proteins are needed to produce infectious virions.
- Among plus-strand RNA viruses, SHFV has the largest number of envelop proteins.

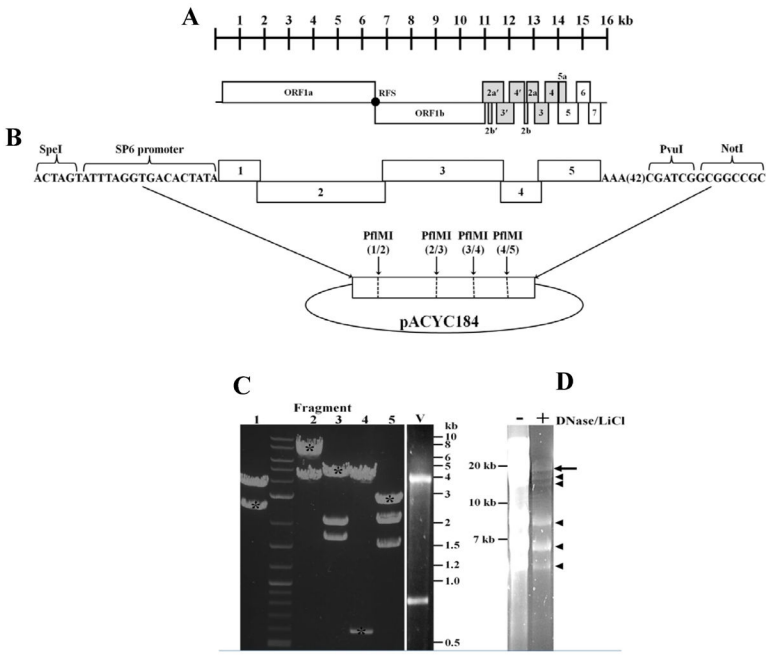

Figure 1. Construction of a full-length SHFV-LVR cDNA infectious clone

(A) SHFV genome organization. The ORFs of the 15.7 kb SHFV genome are indicated by boxes. ORF1a and ORF1ab encode the nonstructural proteins. The 1ab polyprotein is produced when a -1 ribosomal frameshift (RFS) occurs at a slippery sequence. The 3′ ORFs include two duplicated sets of minor structural protein ORFs (gray), ORF5a (gray) and three major structural protein ORFs (white). The minor structural protein ORFs are: ORF2a′ (GP2′), ORF2b′ (E′), ORF3′ (GP3′), ORF4′ (GP4′), ORF2a (GP2), ORF2b (E), ORF3 (GP3), and ORF4 (GP4). The major structural protein ORFs are: ORF5 (GP5), ORF6 (M - membrane protein), and ORF7 (N - nucleocapsid protein). The ORF protein products are indicated in parentheses. ORF5a encodes GP5a which is thought to be an additional minor structural protein. (B) Strategy used for SHFVic assembly. Five overlapping cDNA fragments spanning the genome were generated by RT-PCR and cloned separately into pCR-XL-TOPO. (C) Assembly of the infectious SHFV clone. The five fragment pCR-XL-TOPO clones were cut with PflMI alone (fragments 2 and 4) or also with RsrII (fragment 3), SpeI (fragment 1) or NotI and RsrII (fragment 5). The individual viral genome fragment bands are indicated with an asterisk. The five fragments were simultaneously ligated and cloned into the large capacity vector pACYC184 (V) that had been cut with XbaI and EagI to pair with the SpeI sticky end of fragment 1 and the NotI sticky end of fragment 5, respectively. (D) *In vitro* transcribed viral RNA was incubated with DNase, precipitated with lithium chloride, washed with ethanol and electrophoresed on an RNase-free denaturing 2% agarose gel. An arrow indicates the full-length genome RNA and arrowheads indicate shorter RNA products *in vitro* transcribed from the infectious clone cDNA.

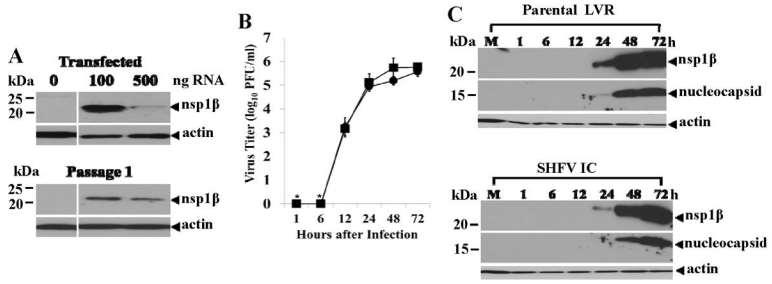

Figure 2. Comparison of the replication kinetics of parental and infectious clone viruses

(A) MA104 cells were transfected with 0, 100 or 500 ng of RNA *in vitro* transcribed from the SHFV infectious clone cDNA. Culture fluid was collected 72 h after transfection and 100 μl were used to infect a fresh MA104 monolayer. Passage 1 culture fluid was harvested after 72 h. Western blots of cell lysates collected 72 h after viral RNA transfection using anti-nsp1β protein antibody. (B) Virus yields produced by MA104 cells infected at an MOI of 1 with either parental or Passage 1 SHFVic virus. Virus yields were quantified by plaque assay on MA104 cells. (■) Parental virus. (●) SHFVic virus. Data points are average values from three independent experiments. Each virus titration was done in duplicate. Error bars represent standard deviation (SD). *-Virus titers in the 1 and 6 h were below detection (<100 PFU/ml). (C) Time course of intracellular nsp1β and nucleocapsid protein production in MA104 infected with parental or SHFVic virus (MOI of 1). Proteins were detected in cell lysates by Western blotting using viral protein specific antibodies. The blots shown are representative of three independent experiments. Actin was used as a loading control.

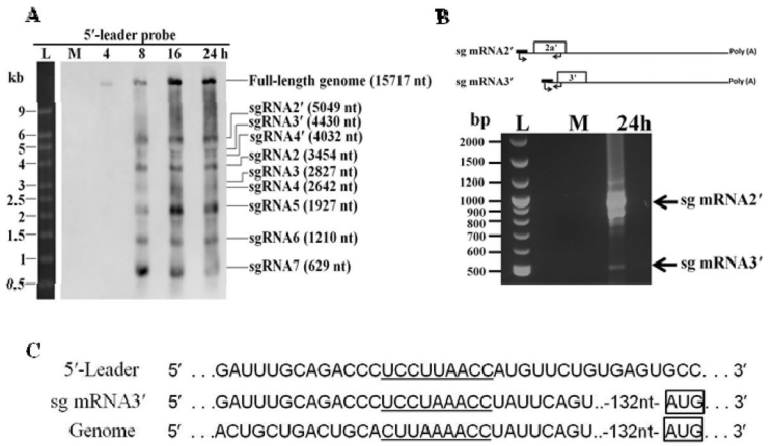

Figure 3. Analysis of sg mRNAs produced by MA104 cells infected with SHFVic virus

(A) Northern blot analysis of viral sg mRNAs. MA104 cells were mock infected (M) or infected with SHFVic virus at an MOI of 1 and total RNA was extracted at 4, 8 16 or 24 h after infection. Cell RNA (1 μg) was electrophoresed on a 1% denaturing agarose gel, transferred to an Hybond-N^+ membrane and hybridized with a DIG-labeled 5′ leader RNA probe. The sg mRNAs were identified based on size. (B) Top-Diagram indicating the positions of the RT-PCR primers used. Bottom- Cell RNA was extracted from MA104 cells 24 h after infection with SHFVic virus at an MOI of 1 and subjected to RT-PCR. The PCR products were separated on a 2% agarose gel. The ~1000 and ~500 bp DNA bands were excised and the extracted DNA was TA cloned and sequenced. (C) The junction sequence for sg mRNA 3′ obtained from the ~500 bp band was aligned with the genome and 5′ leader sequences.

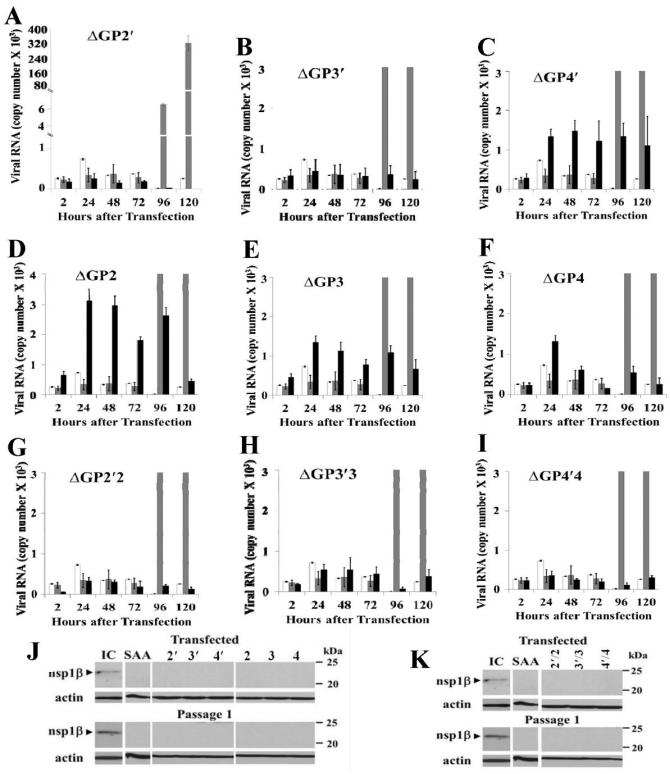

Figure 4. Effects of knocking out the expression of individual minor structural glycoprotein ORFs on extracellular viral RNA levels

(A to J) Analysis of extracellular viral RNA levels. Culture fluids were harvested at the indicated times after transfection of 100 ng of wildtype (gray bars), replication defective SAA mutant (white bars) or (A) ΔGP2′, (B) ΔGP3′, (C) ΔGP4′, (D) ΔGP2, (E) ΔGP3, (F) ΔGP4, (H) ΔGP2′/2, (I) ΔGP3′/3 or (J) ΔGP4′/4 mutant (black bars) *in vitro* transcribed viral RNA. Extracellular viral RNA was extracted from 200 ul of harvested culture fluid and then quantified by qRT-PCR using nucleocapsid region primers and probe and a standard curve generated with a known amount of *in vitro* transcribed viral RNA. Each sample was assayed in triplicate. Error bars represent SD. Values shown are representative of two independent experiments. The complete range of values for the extracellular wildtype viral RNA levels produced is shown only in panel A. (G and K) Western blots done with anti-nsp1β antibody on MA104 cell lysates collected 120 after transfection with the indicated *in vitro* transcribed viral RNA or 120 h after a blind passage infection. The blots shown are representative of data from three independent experiments. Actin was used as a loading control.

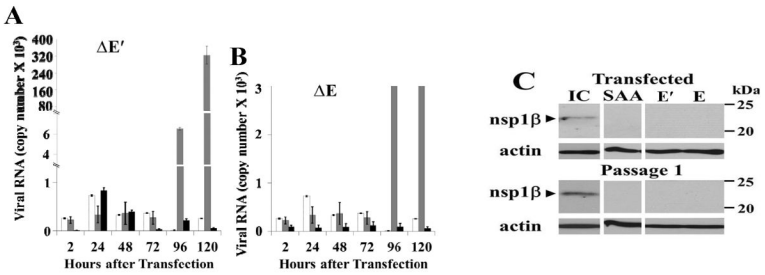

Figure 5. Effects of knocking out the expression of an SHFV E protein ORF on extracellular viral RNA levels

(A and B) Analysis of extracellular viral RNA levels. Culture fluids were harvested at the indicated times after transfection of 100 ng of wildtype (gray bars), replication defective SAA mutant (white bars) or (A) ΔE′ or (B) ΔE mutant (black bars) *in vitro* transcribed viral RNA. Extracellular viral RNA was extracted from 200 ul of harvested culture fluid and then quantified by qRT-PCR using nucleocapsid region primers and probe and a standard curve generated with a known amount of *in vitro* transcribed viral RNA. Each sample was assayed in triplicate. Error bars represent SD. Values shown are representative of two independent experiments. The complete range of values for the extracellular wildtype viral RNA levels produced is shown only in panel A. (C) Western blots done with anti-nsp1β antibody on MA104 cell lysates collected 120 after transfection with the indicated *in vitro* transcribed viral RNAs or 120 h after a blind passage infection. The blots shown are representative of data from three independent experiments. Actin was used as a loading control.

Table 1

Primers used to generate overlapping cDNA fragments from SHFV-LVR RNA.

Primer	Sequence (5′ to 3′)
Fragment 1	
F-SP6-1	act agt ATT TAG GTG ACA CTA TAG ATT AAA ATA AAA GTG TGA AGC[a, b]
R-2343	CAA CCA CCC AAT GGT CAG AGT CAA GG
Fragment 2	
F-2307	TAC GTT GTG CGC CTT GAC TCT GAC
R-7991	GCT TGC CAG ACA GAA ATT TGA GAC TG
Fragment 3	
F-7858	TGG TCT CTC CTC AGG TGA TC
R-12306	AGT CAT GTT GCC TGT AAT TGT CTC
Fragment 4	
F-12190	TAT GTC TAT CGT CCA CCA CTT GTC
R-12983	AGG TAT TTA GAA AGT CCA GTC ACG
Fragment 5	
F-12662	TCT GCT GGT TGG TAA AAT GCT CTC ACT CAC
R-15717	gcg gcc gcc gat cgt $(T)_{42}$ AAT TAT GGT ATA[b]

[a] SP6 promoter consensus sequence is indicated by underlining.

[b] Recognition sites for restriction enzymes SpeI in R2343 and NotI and PvuI in R-15717 are in lowercase.

Table 2

Primers used to make the minor structural protein knockout mutants

ORF(gene)		Primer sequence (5′ to 3′)
ORF2a′ (GP2′)	F	CCCTCTCCTCTGcTGAGTTTCTGTCCAGG
	R	CCTGGACAGAAACTCAgCAGAGGAGAGGG
ORF2b′ (E′)	F	CACTTCTCCTCCTCCTTCAAGTACTAcGATCACACCCACATTCATACTG
	R	CAGTATGAATGTGGGTGTGATCgTAGTACTTGAAGGAGGAGGAGAAGTG
ORF3′ (GP3′)	F	GAAGGAGAGTTCTGTACCcTGGTTTCAACTTGGTTTC
	R	GAAACCAGATTGAAACCAgGGTACAGAACTCTCCTTC
ORF4′ (GP4′)	F	CCTAACAATCAAGCAATCcTGGAACGAGACAATGATG
	R	CATCATTGTCTCGTTCCAgGATTGCTTGATTGTTAGG
ORF2a (E)	F	GCCTTCCACCAcGCTGTCCACGAGCTCC
	R	GGAGCTCGTGGACAGCgTGGTGGAAGGC
ORF2b (GP2)	F	CGATCTTTAGAGCATTCTATTCTTAgTGGGTTCTATACTCACCCACATC
	R	GATGTGGGTGAGTATAGAACCCAcTAAGAATAGAATGCTCTAAAGATCG
ORF3 (GP3)	F	CAGTTATCTCACTAACCCcTGGATGTCCGTGG
	R	CCACGGACATCCAgGGGTTAGTGAGATAACTG
ORF4 (GP4)	R	CCAGTTTGATAACGAGACATTcTGCTACATTGCAAACCTTAC
	F	GTAAGGTTTGCAATGTAGCAgAATGTCTCGTTATCAAACTGG

Effects of the mutations on an overlapping ORF

CTCTGcTGAGT (ORF2a′): ATG to CTG (knock out start codon)

TACTAcGATCA (ORF2b′): ATG to ACG (knock out start codon)

TACTAcGATCA (ORF2a′): TAT to TAC (Tyrosine to Tyrosine)

GTACCcTGGTT (ORF3′): ATG to CTG (knock out start codon)

GTACCcTGGTT (ORF2a′): CCA to CCC (Proline to Proline)

CAATCcTGGAA (ORF4′): ATG to CTG (knock out start codon)

CAATCcTGGAA (ORF3′): TCA to TCC (Serine to Serine)

CACCAcGCTGT (ORF2a): ATG to ACG (knock out start codon)

CACCAcGCTGT (ORF2b): CAT to CAC (Histidine to Histidine)

TCTTAgTGGGT (ORF2b): ATG to GTG (knock out start codon)

TCTTAgTGGGT (ORF4′): TAA to TAG (STOP codon to STOP codon)

AACCCcTGGAT (ORF3): ATG to CTG (knock out start codon)

AACCCcTGGAT (ORF2): CCA to CCC (Proline to Proline)

ACATTcTGCTA (ORF4): ATG to CTG (knock out start codon)

ACATTcTGCTA (ORF3): TTA to TTC (Leucine to Leucine)

Table 3

Primers used to generate a 5′ leader probe and for sg mRNAs 2′ and 3′ amplification.

Primer	Sequence (5′ to 3′)
5'-leader-probe-F	AATAAAAGTGTGAAGCTCCCTGTGCTTTCATGCCAGG
5'-leader-probe-R	CGGTAGTAATACGACTCACTATAGGGTCTGCAAATCCCAAGCCAC
5'-Leader-RTPCR-F	TAGCCCGGATTGGATAAGC
sg mRNAs2′ and 3′-RTPCR-R	CGTAGGTGAGAATGATGG

Table 4

Nucleotide differences between the GenBank (AF180391.1) and the SHFVic

Position	GeneBank	New sequencing	Amino Acid Change	Gene
511	C	T	P101L	nsp1α
849	G	T	V214F	nsp1β
1658	G	A	silent	nsp1γ
2503	G	C	G765A	nsp2
3726	C	-	10 aa frame shift	nsp2
3757	-	A	10 aa frame shift	nsp2
3785	A	G	silent	nsp2
4277	T	G	silent	nsp3
4895	A	G	silent	nsp4
5575	G	T	G1889V	nsp5
5695	G	A	R2018H	nsp5
5704	A	T	L2021I	nsp6
5707	C	G	P2022R	nsp6
5727	A	T	I2029F	nsp6
6088	G	C	G1960A	nsp7
8276	T	G	S2879A	nsp9
8340	G	T	W2900L	nsp9
10359	T	C	L3373S	nsp11